Received 28 January, 2021; revised 3 March 2021; accepted 6 March 2021. Date of publication 19 March 2021; date of current version 22 April 2021.

*Digital Object Identifier 10.1109/OJAP.2021.3067471*

# Dual-Polarized High-Isolation Antenna Design and Beam Steering Array Enabling Full-Duplex Communications for Operation Over a Wide Frequency Range

**MAKSIM V. KUZNETCOV [1] (Graduate Student Member, IEEE), SYMON K. PODILCHAK [2] (Member, IEEE), ARIEL J. MCDERMOTT [1] (Student Member, IEEE), AND MATHINI SELLATHURAI [1] (Senior Member, IEEE)**

[1]Sensors, Signals, and Systems, Heriot-Watt University, Edinburgh EH14 4AS, U.K.

[2]Institute of Digital Communications, The University of Edinburgh, Edinburgh EH9 3JW, U.K.

CORRESPONDING AUTHOR: M. SELLATHURAI (e-mail: m.sellathurai@hw.ac.uk)

This work was supported in part by the U.K. Engineering and Physical Sciences Research Council under Grant EP/P009670/1.

**ABSTRACT** A new dual-polarized antenna and array are presented for In-Band Full-Duplex (IBFD) applications, offering high inter-port isolation. The single-element antenna system consists of four H-shape slots, stacked patches for wide bandwidth, and two external hybrid couplers. The multilayer antenna is well matched from about 2.1 to 2.4 GHz and provides high isolation in this frequency range in excess of 60 dB. Two different prototypes are simulated and measured to highlight the design process. In addition, a new and compact hybrid coupler with excellent phase and magnitude stability is also presented for improved antenna radiation and IBFD performances. When compared to other similar types of hybrid coupler and antenna systems, the proposed configurations are simple to manufacture, provide a higher isolation bandwidth (10%), and higher gain of 7.3 dBi with cross-polarization levels of 30 dB or lower. The single-element design was also extended to a $2\times2$ array and studied for different beam steering and feeding scenarios. The operating bandwidths and isolation values offered by these S-band antenna and array systems can support new data link possibilities for beam steering and future low-cost IBFD wireless networks by simple antenna fabrication.

**INDEX TERMS** Dual-polarization, double-differential antenna, full duplex, isolation, simultaneous transmit and receive (STAR).

## I. INTRODUCTION

WITH the advancements of wireless communications, full-duplex (FD) antenna systems are once again a topic of interest [1]. These systems are attractive not only because of their ability to simultaneously transmit and receive thus requiring less antenna hardware, but also, due to the possibility of increased channel capacity and spectrum density [2]–[4]. However, due to this simultaneous transmit and receive capability, these systems can experience high self-interference (SI) where the transmitted signal is so strong that it suppresses the received signal making FD data transmission challenging.

One of the first implementations of FD systems was in radar. Due to technological limitations, the only way to reduce interference was to control the transmitting power which causes the operating range of the radar to be limited. With more recent advances, there are now a number of technologies that can be employed to suppress this interference. One way to cancel out the SI is to implement an analogue cancellation mechanism, for example, using coupler phase compensation systems to cancel out the received signal or expensive and bulky circulators which might have only 20 or 40 dB of isolation [5], [6]. Another method of SI suppression is digital cancellation. Examples of digital cancellation

techniques are the use of specific transmission protocols [7] or digital-domain cancellation [8]. Finally, one of the most efficient and low-cost means of SI suppression is to adopt antenna-related approaches for signal isolation. This could be the utilization of different frequencies for up-link and down-link data transmission (dual-band) [9], or if a single frequency (in-band) is required, a dual-polarized antenna with high port-to-port isolation might be preferred [10]. Both approaches can support FD communications.

Depending on the application, these techniques can be combined or employed to suppresses the SI to the required level. Typical examples of isolation values that have been reported in the literature are in the order of 70 to 80 dB [11] over a bandwidth of 3%. To achieve good FD operation [12], with a bit-error-rate (BER) suitable for robust two-way communications, the total SI cancellation must be approximately 100 dB [12] or higher (reaching the noise floor of the system). For example, in [11] and [13], isolation values in excess of 100 dB were reported when using FPGA digital cancellation, circulator-based antennas, and analogue circuit cancellation.

One of the earliest designs of an inter-port antenna with high isolation was a circular patch design in [14]. In that paper, two antenna designs were investigated. Both consisted of two H-shaped slots and circular shaped patches elevated above the ground plane. As a result, the antennas offered bandwidths of 8% with isolation values of only 31.3 dB. In that same work [14] the authors extended the system to four H-shaped slots and a feeding circuit consisting of two Wilkinson power dividers. Using this approach, the authors were able to improve the antenna bandwidth to 17% and the port-to-port isolation to 34 dB. The antenna gains reached 6.8 dBi with cross-polarization levels of 14 dB at the center frequency.

Another method to achieve high isolation between the transmitting and receiving ports is to design a Dual-Band (Out-of-Band) system. Antennas in such systems are less affected by SI due to having different transmitting and receiving frequencies. One such antenna was proposed in [9]. In that design the data was transmitted at a center frequency of 4.7 GHz and a received frequency of 6 GHz. The antenna consisted of coupled-resonators with a patch placed on top. The reported antenna $-10$ dB impedance bandwidth was about 5.5% with isolation values around 35 dB and a maximum gain of 6.7 dBi. The antenna was further expanded into a $2\times2$ array system which slightly reduced the isolation to 30 dB and increased the gain to a maximum of 12 dBi. In a similar fashion, the dual-polarized antenna reported in [15] utilized a four-port system to achieve dual-band operation at 1.8 GHz and 2.0 GHz for transmitting and receiving, respectively. The proposed antenna consisted of resonator-based filtering channels, slot lines, and a radiating patch. The reported gain was 7.2 dBi and the isolation was greater that 23 dB.

Following these recent developments, in-band full-duplex (IBFD) antennas are generally of greater interest than their dual-band counterparts, for reasons of their single frequency re-use and doubled spectral efficiency [16]. The main focus of recent research studies was to achieve wider bandwidths, high as possible inter-port isolation, and to operate using dual-polarization. Previous FD antennas, which operate over a wide frequency range, as proposed in the literature are generally complex, might require careful feed and design considerations, and possibly can be expensive to manufacture. One such antenna was proposed in [17]. The involved design consisted of four T-shape parasitic elements mounted on a metallic ground plane. However, the antenna provided an impressive bandwidth of 98% and operated at frequencies between 0.6 to 1.75 GHz with isolation values below 40 dB. Maximum realized gain for the receive and transmitting mode was approximately 7 dBi and 6 dBi, respectively, and with an omnidirectional-like radiation pattern. Similarly, a metallic-based, four-port antenna was reported in [18]. It provided an wider bandwidth of 108% and operated from 0.8 GHz to 2.7 GHz. The antenna design consisted of resonating metallic ring elements with dipole-like arms, producing a monopole-like radiation pattern. The reported maximum realized gain was 7 dBi with inter-port isolation values of 37 dB over the entire operating range.

These antennas are suitable for use in base station applications due to their wide operational bandwidth and their physical size. However, simpler and lower-cost solutions using printed circuit board (PCB) manufacturing techniques, for example, can be more attractive for use in more basic or low-power radio transmission links for day-to-day communication systems such as Wi-Fi.

Recently, different structures have been reported which consist of hybrid couplers and a single resonating patch antenna [19], [20]. These designs are based on a single- and double-differential signal shift, where a phase shift of 180° is achieved between two coupler ports while a third port is terminated by a 50-Ω load. With this feeding, SI is reduced and a high isolation of 40 to 50 dB can be achieved whilst the antenna system is matched. Moreover, due to the signal cancellation effect at the coupler, i.e., the 180° phase shift, the antenna cross-polarization in the far-field is also improved. However, previous designs [19], [20] which have implemented this technique have offered narrow isolation bandwidths. On the other hand, the antenna presented in [21], which operated at 5 GHz, achieved isolation levels of over 50 dB with a bandwidth of about 9%. That antenna system [21] was implemented using only one slot-line type hybrid coupler supported by a network of power dividers making it a single-differential feeding approach. In that work, port one of the coupler provided an equal signal phase shift, while port two provided a differential shift. This possibly limited the antenna performance and increased the cross-polarization levels. Moreover, the $-10$ dB impedance bandwidth over frequency for ports 1 and 2 were not the same.

Another IBFD dual-CP antenna based on a sequential rotation array (SRA) and an additional phase compensation control circuit was proposed in [22]. The system consisted of four circularly polarized patches, two 180° hybrid couplers,

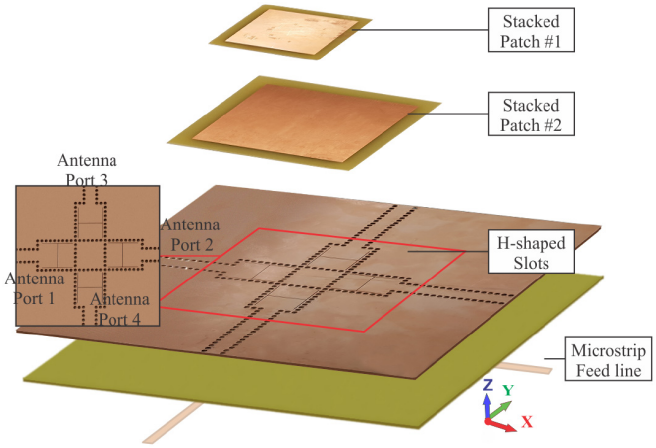


**FIGURE 1.** Antenna design exploded view: four-port antenna system with H-shaped slots and two parasitic square patch elements on top to increase bandwidth. Two external couplers are required (as in Fig. 2) to enhance the isolation.

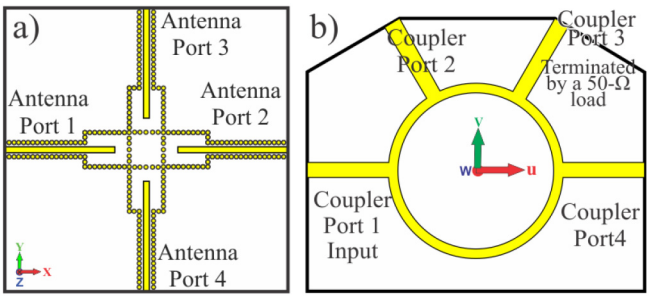


**FIGURE 2.** Bottom view of the feed system and coupler layout. a) Bottom view: 50-Ω microstrip lines are printed on the bottom to feed the H-shaped slots which are isolated using vias. b) Rat-Race coupler: Coupler Port 1 is the input port to the antenna and feeding network and system, Coupler Ports 2 and 4 are connected using external cables to Antenna Ports 1 and 2 to provide a 180° phase shift; i.e., differential feeding while Coupler Port 3 is terminated with a 50-Ω load. A second coupler and analogous connections are required for Antenna Ports 3 and 4.

and an additional circuit on the receiver port with an attenuator and phase shifter. The reported radiation bandwidth was 10% with a maximum realized gain of 10 dBic. In addition, the developed cancellation circuit on the receiver side, integrated on a separate board, compensated the phase instabilities of the cables and the hybrid coupler. This improved the isolation beyond 50 dB.

Following these developments we propose a new and low-cost antenna and array offering high inter-port isolation which can be useful for future wireless networks and RF-IBFD systems. Our design process is reported in Sections II and III. By the inclusion of simple antenna excitation approaches for improved bandwidths, double-differential feeding, and by adopting different isolation techniques not explored previously in the literature for FD antennas, the problem of SI can be further alleviated whilst offering an advancement from previous studies. For example, isolation values in excess of 60 dB are observed for a corresponding 10% impedance bandwidth for the developed antenna (see Figs. 1 and 2). To explore the design attributes and to report our findings, a few prototypes are simulated and measured. In addition, a new and compact slot-line coupler with high phase and magnitude stability is also developed (see Section IV) for improved IBFD antenna and system performances. Concepts are further expanded to a 2×2 array for IBFD beam steering applications in Section V while some concluding remarks are stated in Section VI. To the best knowledge of the authors, no similar single-element, compact slot-line coupler, and antenna array have been previously reported.

**TABLE 1.** Prototype comparisons considering the cables and couplers.

| Developed Prototype | Measured / Simulated | Frequency Range | Percentage Bandwidth | Corresponding Isolation Range |
|---|---|---|---|---|
| Foam Spacer | Simulated | 2.15 to 2.34 GHz | 10% | 45 to 49 dB |
| Foam spacer | Measured | 2.15 to 2.35 GHz | 9% | 48 to 49 dB |
| Nylon Screws | Simulated | 2.25 to 2.45 GHz | 10% | 60 to 70 dB |
| Nylon Screws | Measured | 2.14 to 2.42 GHz | 11% | 48 to 60 dB |

## II. ANTENNA DESIGN, SIMULATIONS, AND GENERAL CONSIDERATIONS FOR THE SINGLE-ELEMENT

The proposed IBFD antenna consists of four H-shaped slots connected to 50-Ω microstrip lines and two parasitic patch antennas placed on top of the slot arrangement (see Figs. 1 and 2(a)) for improved bandwidth. Initially two Rat-Race couplers, as in Fig. 2(b), were included for the simulated antenna feeding system and the elevated patches were positioned with no mechanical fixtures. Then foam spacers and nylon screws were included defining the first and second prototypes, respectively. The antenna design dimensions can be seen in Fig. 3 and Table 2 for the structure using foam with simulations and measurements in Figs. 4 to 8. A photo of the second prototype using nylon screws is also shown in Fig. 9. Both the foam spacer and the nylon screw-based designs are compared in this paper to understand the benefits of the different structures as well as to outline the design evolution to a final single-element which can offer significantly better IBFD antenna operation when compared to other structures as found in the literature. See Tables 2 and 3 where results are compared in terms of bandwidth, isolation, cross-polarization levels, and manufacturing simplicity.

To reduce leakage effects and improve the isolation, the H-shaped slots in both designs were surrounded by a network of metalized vias (see Fig. 9) with a diameter and periodicity of 2 mm and 3.3 mm, respectively. The antenna PCB design material was FR-4 (see Fig. 1, for stacked patch # 1 and # 2) with a relative permittivity of 4.6 and thickness of 1.6 mm. The H-shaped slots serve as an excitation mechanism for the top radiating patches [23] with square dimensions of 48.3 mm for the bottom patch and 42.5 mm for the top patch. This multilayer configuration can increase the bandwidth of the antenna system. The overall dimensions of the system are 150 mm by 150 mm (which corresponds to 1.13 $\lambda_0$ by 1.13 $\lambda_0$ at the lowest operating frequency of 2.25 GHz, where $\lambda_0$ is the free-space wavelength). The choice of the relatively large ground plane size increases the antenna gain whilst reducing the sidelobe levels (SLLs) caused by any parasitic radiation from the H-shaped slots.

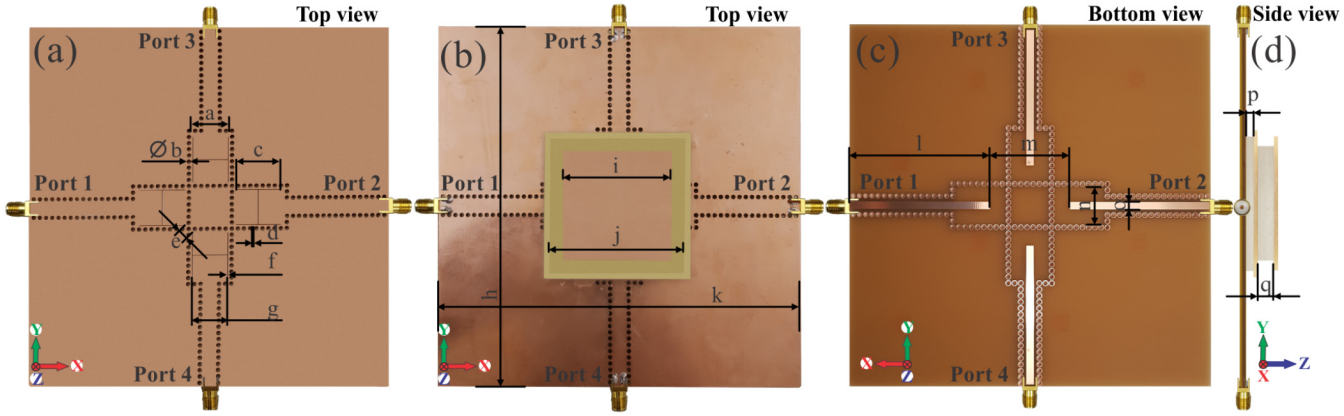


**FIGURE 3.** Fabricated antenna design considering foam spacers (see dimensions in Table 2): (a) top view: four H-shaped slots with embedded vias. (b) Top view: loaded parasitic patches on top of the four H-shaped slots. (c) Bottom view: four 50-Ω lines with connectors. (d) Side view: two parasitic patches and the foam placed in between.

**TABLE 2.** Antenna dimensions as outlined in Fig. 3 (all values in millimeters).

| $a$ | $b$ | $c$ | $d$ | $e$ | $f$ | $g$ | $h$ | $i$ | $j$ | $k$ | $l$ | $m$ | $n$ | $o$ | $p$ | $q$ |
|---|---|---|---|---|---|---|---|---|---|---|---|---|---|---|---|---|
| 16 | 2 | 19 | 1.3 | 4.3 | 0.2 | 14.6 | 150 | 42.5 | 51.7 | 150 | 58.3 | 33.3 | 14.6 | 3.1 | 4.2 | 9.4 |

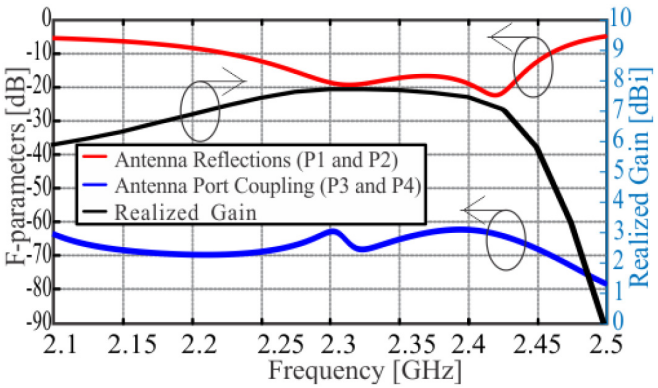


**FIGURE 4.** Simulated antenna F-parameters from CST considering 0° and 180° phase shifts applied to Antenna Ports 1 and 2, respectively (see Figs. 1 and 2). Similar results are observed when applying analogous feeding to Antenna Ports 3 and 4, but with an opposite polarization for the radiated far-fields. Realized gain values approach 8 dBi (see right axis).

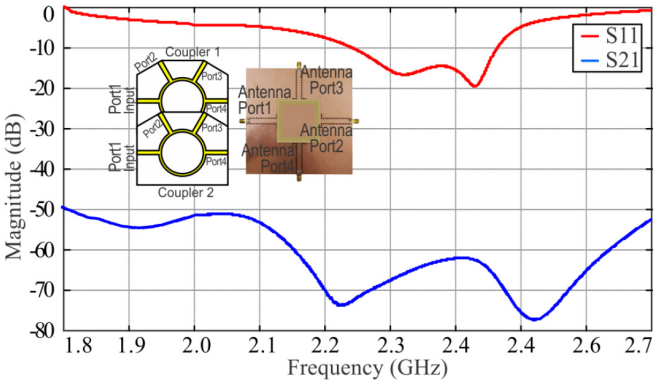


**FIGURE 5.** Simulated ideal antenna (air spacing for the patches whilst considering dielectric substrate losses, and ideal connections; i.e., no physical cable connections) response with the external coupler system (see Fig. 2). Antenna Ports 1 and 2 where connected to Ports 2 and 4 of Coupler 1. Likewise Antenna Ports 3 and 4 where connected to Ports 2 and 4 of Coupler 2. The $|S_{11}|$ is the port reflection coefficient at Port 1 of Coupler 1 (analogous results were observed for Coupler 2). The plotted $|S_{21}|$ is the coupling between Coupler 1 and Coupler 2 (connected to Port 1 for both). Port 3 of both couplers are loaded with 50-Ω.

As a first step in the feeding system design a basic microstrip-based hybrid coupler was employed (see Fig. 2). This enables double-differential external feeding making the feeding network for the single-element consist of two simple Rat-Race couplers. These couplers were designed and manufactured using a Taconic TLY-5A substrate which has a relative permittivity of approximately 2.2 and a thickness of 1.6 mm. With this external feeding approach, the two driven Antenna Ports (1 and 2, or 3 and 4, see Figs. 1 and 2) will have a 180° phase shift. This antenna and feed configuration can provide two orthogonal linear polarizations with a main beam radiating at broadside. For example, by driving Antenna Ports 1 and 2, the generated far-fields in the *x*-*z* plane will be linearly polarized. Similarly, by exciting antenna ports 3 and 4, the dominant fields in the *y*-*z* plane will also be linearly polarized. Moreover, when the two couplers have perfect phase balance and the same amplitude; i.e., minimal magnitude imbalance, the inter-port leakage of the transmitted and the received signal can be minimized.

The antenna and hybrid couplers were designed and simulated in the commercial full-wave simulator CST microwae studio. Since the antenna ports will be driven simultaneously, the proposed structure was initially optimized and analyzed using active F-parameters (i.e., active S-parameters), with the applied 0° and 180° shifts and without the external hybrid coupler system. Simulations suggest that the antenna is well matched between about 2.2 GHz to 2.46 GHz where the reflection coefficient is below −10 dB. Also, the corresponding port isolation is below 60 dB in this frequency range (see Fig. 4). This defines an operating bandwidth of about 10%. The simulated maximum realized gain can be observed at 2.3 GHz in Fig. 4 with a value of 7.8 dBi. Also, the antennas and couplers were simulated independently which allowed us to use the S-parameter combination tool in CST. Isolation values of more than 70 dB over the operating frequency

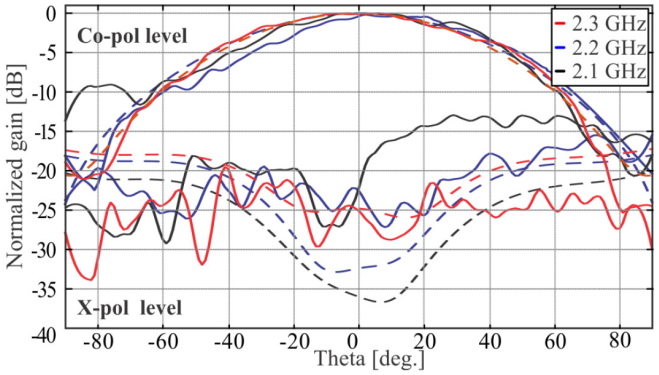


**FIGURE 6.** Simulated (dashed lines) and measured (solid lines) normalized beam patterns at the operating frequencies for the antenna as in Fig. 3. Results are in agreement and cross-polarization levels are 20 dB (or more) below the main beam at boresight.

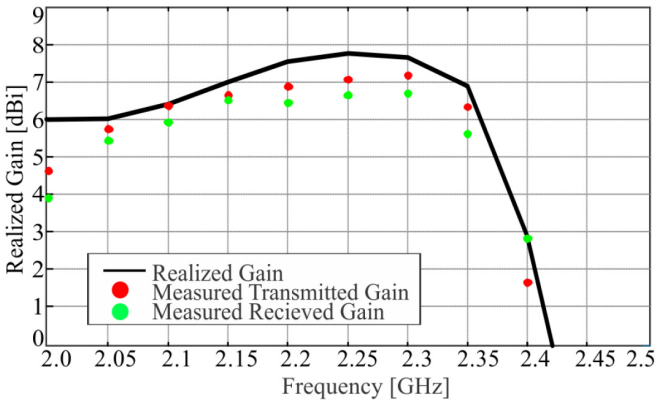


**FIGURE 7.** Simulated (black line) and measured (red/green dots) realized gains for the antenna system considering foam spacers (see Fig. 3). It should be noted that the single-element was measured in both transmit and receive mode.

range of the antenna and coupler system can be observed (see Fig. 5).

## III. SINGLE-ELEMENT FABRICATION AND SYSTEM MEASUREMENTS

The proposed prototype IBFD antenna and cuplers were manufactured and measured. A photograph of the antenna prototype with foam spacers and nylon screws can be seen in Figs. 3 and 9, respectively. The S-parameter measurements were done using Keysight PNAs N5225A and 5234A. The antenna was loaded with the elevated patches. Ideally the H-shaped slots and the patches would by spaced apart by air layers. For implementation of the first prototype, Laird Eccostock PP-4 type foam with a relative permittivity of 1.06 was used as a spacer between the patches and the H-shaped slots.

To verify the beam pattern performance in the far-field, the antenna measurement system DAMS 7100 Diamond Engineering was used in the anechoic chamber at Heriot-Watt University. As a reference antenna, a Flann Horn (type 08240) was employed. The simulated and measured beam patterns can be observed in Fig. 6 while the antenna gain (measured in both receive and transmit modes) is reported in Fig. 7. It should be mentioned that the maximum measured

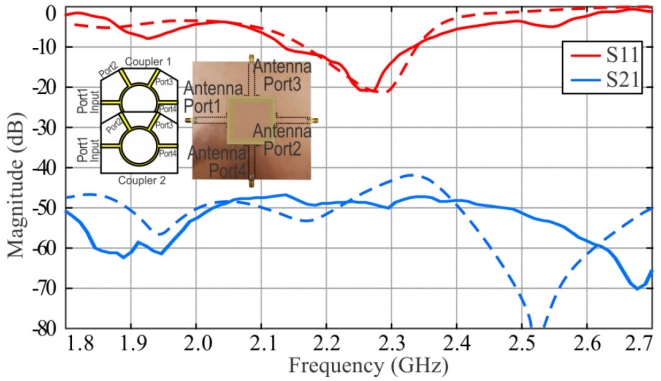


**FIGURE 8.** Simulated (dashed lines) and measured (solid lines) S-parameters of the antenna with the couplers and cables (foam spacer design, Fig. 3). In particular, the S-parameter combination tool in CST was employed which included simulation and measurement results of the couplers, the phase matched cables, and the four-port antenna. This provided the combined simulation and measurements of the final two-port antenna system.

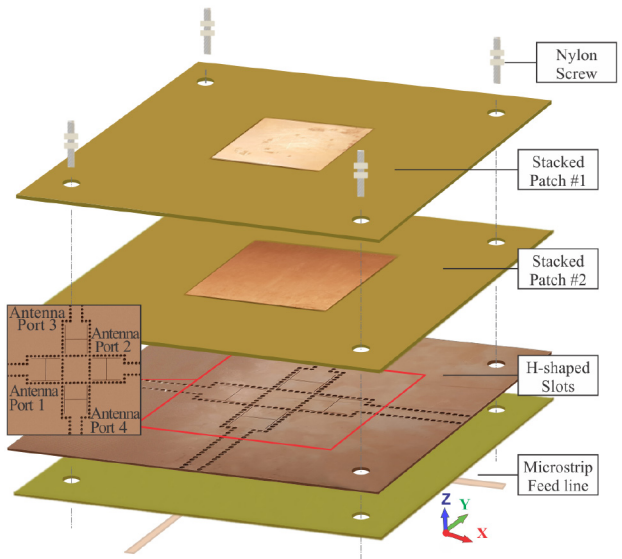


**FIGURE 9.** Exploded view of the antenna prototype design (using nylon screws).

realized gain was 7.3 dBi at 2.3 GHz, which is slightly less than what was simulated by about 0.5 dBi. Measured realized gain from ports one and two, and three and four, are similar since the antenna is fully symmetrical. However, in receive mode the measured gain was slightly lower. These minor discrepancies could be related to measurement tolerances or interactions with the antenna positioner. Regardless, the normalized beam patterns for the operating frequencies can be seen in Fig. 6 which match the simulations. Measured cross polarization levels are more than 20 dB from the main beam maximum at broadside.

Subsequent simulations which took into account the foam materials, some possible misalignments, and other fabrication tolerances showed that the frequency was shifted by about 50 MHz which better matched the S-parameter measurements (see Fig. 8). Due to these practicalities the inter-port isolation was reduced by about 5 to 10 dB over

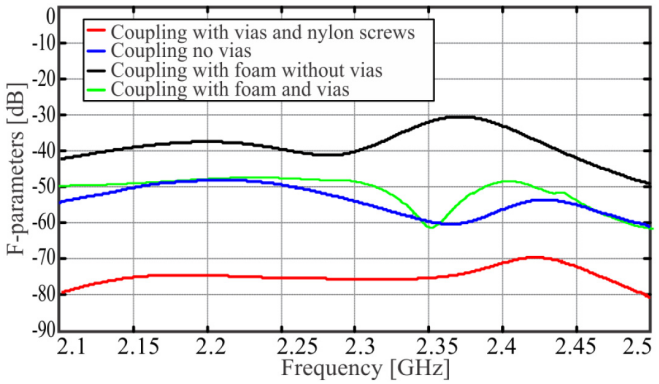


**FIGURE 10.** Simulated F-parameter coupling of the antenna designs considering different isolation techniques (see legend) and common design features. In these simulations no external feeding systems were considered.

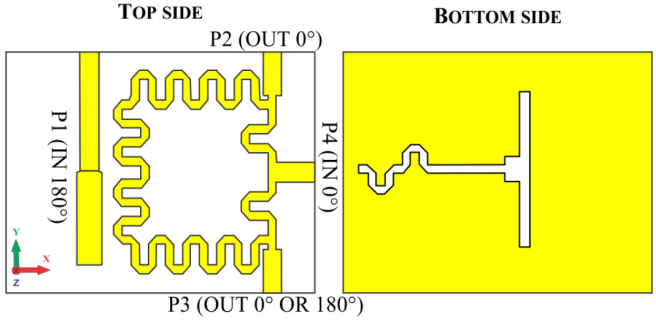


**FIGURE 11.** Top and bottom view of the proposed slot-line meandered hybrid coupler. It should be noted that the coupler can operate as a 0° divider when port 4 is driven. However, when port 1 is excited, a 180° phase difference can be observed at ports 2 and 3.

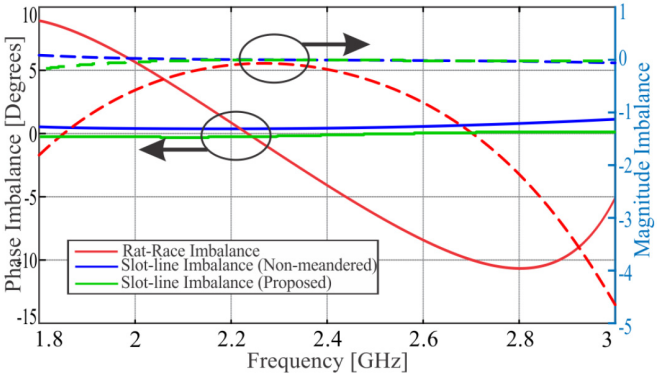


**FIGURE 12.** Simulated phase and magnitude imbalances (active ports for a 180° phase shift) of the hybrid couplers: Rat-Race type (considered for the single-element antenna, Fig. 2) as well as the non-meandered and the proposed compact, meandered slot-line type (see Fig. 13). It can be seen that the slot-line coupler has less than a 0.5° phase imbalance and a 0.2 dB magnitude imbalance.

the frequency range of interest. To circumvent this practical design challenge and improve the isolation, the second antenna prototype was optimized and manufactured using nylon screws with extended substrate layers for the top patches. This helped to improve the alignment and positioning of the various layers (see Fig. 9). The antenna F-parameters were simulated to validate the coupling of these approaches as reported in Fig. 10. It can be observed that the antenna with the nylon screws and vias provided the best isolation suggesting structure fabrication and further testing.

During the measurements of these antenna systems, it was also observed that the phase matched cables and port connectors (which where made consistent for all antennas), introduced additional phase imbalances, which likely resulted in reduced isolation levels between the antenna ports. The full system S-parameter simulations and measurements including the cables, the couplers, and the antenna for the foam prototype are presented in Fig. 8 with results for both structures in Table 1. In these measurements two short low-loss (phase-matched) cables were used. It is important to note that due to the long 50-Ω microstrip feeding lines, coaxial cables were required to feed the signals to the coupler ports. These additional cable lengths and the required connector ports, which is not possible to avoid with the external couplers, introduced some practical phase and magnitude imbalances and reduced port-to-port isolation.

It is also important to note that at low frequencies the environmental noise could also be problematic (even in a fully enclosed anechoic chamber) when trying to achieve low isolation responses which are inline with the simulations (all results not reported for brevity). Regardless, from the simulations and measurements, the antenna with nylon screws provided a similar response, but with improved isolation as outlined in Table 1. For example, the measured isolation range, when the antennas are matched (i.e., the external port reflection coefficients are −10 dB or less), is higher than 49 dB and 60 dB for the antenna prototype with foam spacers and nylon screws, respectively.

Overall, the prototypes show that the measurements and simulations are in agreement when all the cables and couplers where taken into consideration. Some comparisons to other types of IFBD antennas are presented in Table 3, were it can be observed that the single-element can provide some benefits over the existing FD antennas in terms of simplicity and low-cost manufacturing, while maintaining a better operating bandwidth whilst providing high levels of isolation.

## IV. SLOT-LINE COUPLER FOR PHASE STABILITY AND IMPROVED FULL-DUPLEX ANTENNA OPERATION

During the design work as outlined in the previous section, it was realized that antenna operation could be improved when required for FD systems. One such improvement could be the integration of a slot-line based coupler to replace the Rat-race coupler. This is because it is generally well known that microstrip transmission lines are dispersive and that Rat-Race couplers can be relatively narrow band. On the other hand, slot-based structures are less dispersive [27]. The inclusion of a slot-based coupler would reduce the phase imbalances introduced to the antenna by the feeding network. Such imbalances can be seen in Fig. 6 where the beam pattern measurements are slightly squinted and the cross-polarization is higher than simulated.

**TABLE 3.** Comparison to other high isolation antennas found in the literature.

| Reference | Frequency | [1]Impedance Bandwidth | Cross-pol. at Boresight | [2]Corresponding Isolation Range | Element Size (Lowest Freq.) | Ground Plane Size (Lowest Freq.) | Max Gain (Realized) | Feeding Technique | Polarization | Single-element or Array | Multilayer |
|---|---|---|---|---|---|---|---|---|---|---|---|
| [10] | 2.3 to 2.7 GHz | 16% | <-20 dB | 37 to 45 dB | 0.36 by 0.36 $\lambda_0$ | N/A | 8 dBi | - | dual-LP | Planar (Single) | Yes |
| [17] | 0.5 to 2 GHz | 98% | <-10 dB | 40 to 55 dB | 3.5 by 3.5 $\lambda_0$ | 6 by 6 $\lambda_0$ | 5.5 dBi | - | dual-LP | Metal (Array) | Yes |
| [19] | 2.45 to 2.55 GHz | 4% | <-20 dB | 40 to 75 dB | 0.22 by 0.22 $\lambda_0$ | N/A | 4.4 dBi | Single-Diff. | dual-LP | Planar (Single) | No |
| [20] | 2.38 to 2.43 GHz | 2% | <-50 dB | 72 to 98 dB | 0.23 by 0.23 $\lambda_0$ | 1 by 0.67 $\lambda_0$ | 4 dBi | Double-Diff. | dual-LP | Planar (Single) | No |
| [21] | 4.75 to 5.18 GHz | 9% | <-20 dB | 50 to 58 dB | N/A | 3 by 2 $\lambda_0$ | 10.5 dBi | Single-Diff. | dual-LP | Planar (Array) | No |
| [22] | 2.4 to 2.5 GHz | 4% | <-30 dB | 50 to 65 dB | 0.3 by 0.3 $\lambda_0$ | 1.6 by 1.6 $\lambda_0$ | 10 dBic | SRA | dual-CP | Planar (Array) | Yes |
| [24] | 2.25 to 2.6 GHz | 16% | <-25 dB | 41 to 54 dB | 0.32 by 0.32 $\lambda_0$ | 2 by 2 $\lambda_0$ | 10.5 dBic | SRA | dual-CP | Planar (Array) | No |
| [25] | 2.7 to 2.9 GHz | 7% | <-32 dB | 52 to 80 dB | 0.25 by 0.25 $\lambda_0$ | N/A | 5.2 dBi | Double-Diff. | dual-LP | Non-Planar (Single) | Yes |
| [26] | 5.62 to 6.11 GHz | 8.5% | <-20 dB | 35 to 70 dB | 0.21 by 0.15 $\lambda_0$ | 0.85 by 0.75 $\lambda_0$ | 5.8 dBi | - | dual-LP | Planar (Single) | Yes |
| This work - Sim. | 2.25 to 2.45 GHz | 10% | <-27 dB | 60 to 70 dB | 0.32 by 0.32 $\lambda_0$ | 1.13 by 1.13 $\lambda_0$ | 7.8 dBi | Double-Diff. | dual-LP | Planar (Single) | Yes |
| This work - Meas. (Foam) | 2.15 to 2.35 GHz | 9% | <-20 dB | 48 to 49 dB | 0.32 by 0.32 $\lambda_0$ | 1.13 by 1.13 $\lambda_0$ | 7.3 dBi | Double-Diff. | dual-LP | Planar (Single) | Yes |
| This work - Meas. (Nylon) | 2.14 to 2.42 GHz | 11% | <-30 dB | 48 to 60 dB | 0.32 by 0.32 $\lambda_0$ | 1.13 by 1.13 $\lambda_0$ | 7.5 dBi | Double-Diff. | dual-LP | Planar (Single) | Yes |

[1]The transmit and receive ports -10 dB impedance bandwidth (shared bandwidth); i.e. -10 dB impedance bandwidth for ports 1 and 2 of the antenna system.
[2]The corresponding isolation range refers to the external port isolation for the antenna system while the port reflection coefficients are -10 dB (or better).

To improve these results, a slot-based coupler was designed using transmission line meandering for compactness (see Fig. 11). From the simulations of the designed slot-line coupler, the phase imbalance is less that 0.5° while the magnitude imbalance is less than 0.2 dB (see Fig. 12). In the case of Rat-Race couplers, and thus for the antenna design reported in the previous section, it can be observed that the coupler is narrow-band and can only deliver stable operation at the center frequency (see Fig. 12). Moreover, it can be seen that the magnitude imbalances can reach as high as 1 dB while the phase imbalances reach values which are higher than 5°. As described in the following sections, the proposed slot-line based couplers can also be used to improve the phase and magnitude responses as applied to the antenna in transmit and receive mode.

### A. SLOT-LINE COUPLER DESIGN APPROACH USING MEANDERING

One of the earliest slot-line based coupler designs can be found in [28] where magic-T slot-line based stubs were used to control the even and odd modes of operation. Additionally, the structure consisted of coplanar waveguide (CPW) connections and a hybrid-like ring. Using this approach the authors were able to achieve wideband operation from 2.4 to 6 GHz with maximum phase imbalances of 2.5° and a magnitude imbalance of 0.4 dB. Another similar example of such a coupler, but based on microstrip technology can be seen in [29] where a similar magic-T like structure was presented. The placement of the slots above the feeding line provided a stable power split. The authors claimed that by carefully balancing the impedances of the system, by using open stubs and stepped circular rings, the currents can be exploited to enable good operation of the hybrid coupler. The designed structure was able to achieve an almost 80% bandwidth (center frequency of 10 GHz) with maximum magnitude imbalances of 0.25 dB and phase imbalances of 1°. It should also be mentioned that generally slot-line based couplers operate and have better performance at higher frequencies [27].

Advancing on these works we designed a new slot-line/microstrip-based coupler to operate with a 2.3 GHz center frequency. Meandering of the transmission lines was applied for compactness (see Fig. 11). Also, the initial size of the non-meandered coupler was $a = 0.38\ \lambda_0$ by $b = 0.5\ \lambda_0$ (considering lambda at the center frequency of 2.3 GHz). This was reduced to $c = 0.17\ \lambda_0$ by $d = 0.26\ \lambda_0$ (see Fig. 13) for the meandered structure which was fabricated and measured as reported in Figs. 14 to 16.

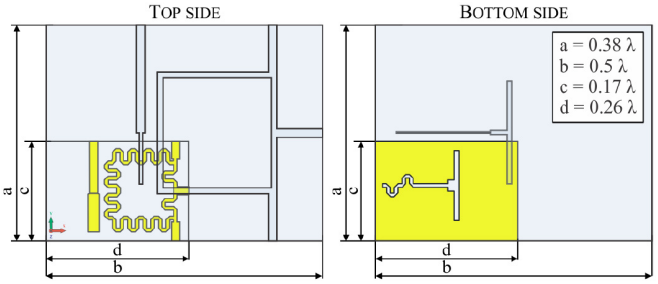


**FIGURE 13.** Size comparison between the meandered and non-meandered couplers. It can be seen that the size is almost three times smaller for the meandered version.

### B. COUPLER PERFORMANCE AND ANTENNA RESULTS

The meandered coupler was designed using CST microwave studio. The reflections for all ports are minimal at port 1 which is matched from 1.9 to 2.6 GHz, and at port 4 which is matched from 2.1 GHz to 3 GHz (see Figs. 15 and 16). The highest magnitude and phase imbalances are around 0.1 dB and 1°, respectively. The isolation between ports 1 and 4 is well below 40 dB. The hybrid coupler was compared to existing devices in the literature (see Table 4) and it can be observed that the developed coupler offers improved compactness, port isolation, and operating bandwidths. These features are important for low-cost, FD antenna systems.

The slot-line coupler was manufactured and measured for the 0° and 180° division input modes (see Fig. 14). For an input into port 1, the coupler divides the signal with the phase shifts of 0° and 180°, while for input into coupler port 4, an equal phase output can be generated. Simulations and measurements are in good agreement. Port 1 is matched from 1.9 to 2.6 GHz while port 4 is matched from 2.1 GHz to 3 GHz (see Figs. 15 and 16). The isolation between ports is also below 40 dB.

The antenna with the foam spacers was simulated considering the phase shifts due to the slot-line and Rat-Race couplers. Results show that the beam tilt and cross-polarization values are improved due to the slot-line coupler (see Table 5).

**TABLE 4.** Comparison of existing hybrid couplers.

| Reference | Center Frequency | Size at Centre Wavelength, $\lambda_c$ | Max Amplitude Imbalance | Max Phase Imbalance | Port Isolation | Impedance Bandwidth (-10 dB) | Transmission Line Technology |
|---|---|---|---|---|---|---|---|
| [29] | 10 GHz | 0.34x0.5 | <0.25 dB | <1° | <29 dB | 70% | Slot-line/Microstrip |
| [30] | 1.4 GHz | 0.29x0.29 | <0.5 dB | <5° | <25 dB | 50% | Microstrip |
| [31] | 14.1 GHz | 2.8x1.8 | <0.24 dB | <1.5° | <30 dB | 18% | Slot-line/SIW |
| [32] | 1.575 GHz | 0.012x0.02 | <0.14 dB | <40.9° | <30 dB | 34% | Balun Type |
| [33] | 2.4 GHz | 0.25x0.25 | <0.5 dB | <5° | <25 dB | 33% | Microstrip |
| This work, Rat-Race | 2.3 GHz | 0.72x0.68 | <4.8 dB | <11° | <15 dB | 66% | Slot-line/Microstrip |
| This work, Non-meandered | 2.3 GHz | 0.38x0.5 | <0.1 dB | <1° | <48 dB | 75% | Slot-line/Microstrip |
| This work, Meandered | 2.3 GHz | 0.17x0.26 | <0.1 dB | <1° | <40 dB | 32% | Slot-line/Microstrip |

**TABLE 5.** Antenna (foam prototype) and coupler response comparison.

| Coupler Type | Beam Position | Frequency | Cross-pol. below Beam Max |
|---|---|---|---|
| Rat-Race | -1° | 2.1 GHz | <-34 dB |
| Slot-line | 0° | 2.1 GHz | <-37 dB |
| Rat-Race | 0° | 2.2 GHz | <-27 dB |
| Slot-line | 0° | 2.2 GHz | <-32 dB |
| Rat-Race | 1° | 2.3 GHz | <-25 dB |
| Slot-line | 0° | 2.3 GHz | <-27 dB |

For example, unwanted beam squints can be observed with the Rat-Race coupler, while improved cross-polarization levels are observed with the slot-line coupler for all cases. Also, when two of these compact, slot-line couplers were used to feed the antenna with nylon screws, measured isolation values were about 50 dB (or better) as shown in Fig. 17. These results demonstrate a clear advantage when using the slot-line couplers in terms of enabling no beam squint over frequency and generally providing lower cross-polarization levels as well as sustained isolation for the practical antenna.

## V. FULL-DUPLEX ARRAY FOR BEAM STEERING APPLICATIONS

The described single-element using nylon screws and the meandered slot-line couplers were employed to design an antenna array system. For 2-D beam steering scenarios, the array configuration was designed to be a 2×2 configuration (see Fig. 18).

The distance between the radiating elements (patches) was 72 mm (0.57 $\lambda_0$ at 2.4 GHz) and the extended ground plane has a total size of 232 mm$^2$. Additionally, to reduce cable length, the feed system was redesigned to provide the shortest transmission line path possible. Unfortunately due to such a feeding approach and array configuration, the integration of vias to improve isolation was not possible due to the proximity of the feeding system to the H-shaped slots. Regardless of these practical challenges the simulated beam patterns show a half-power beamwidth of less than about 35° over the operating bandwidth of the array (see Fig. 19, considering a uniform excitation of the transmitting elements) with cross-polarization levels in excess of 40 dB from the main beam maximum. Also, as reported in Fig. 20 the array is well matched from about 2.15 GHz to 2.4 GHz while

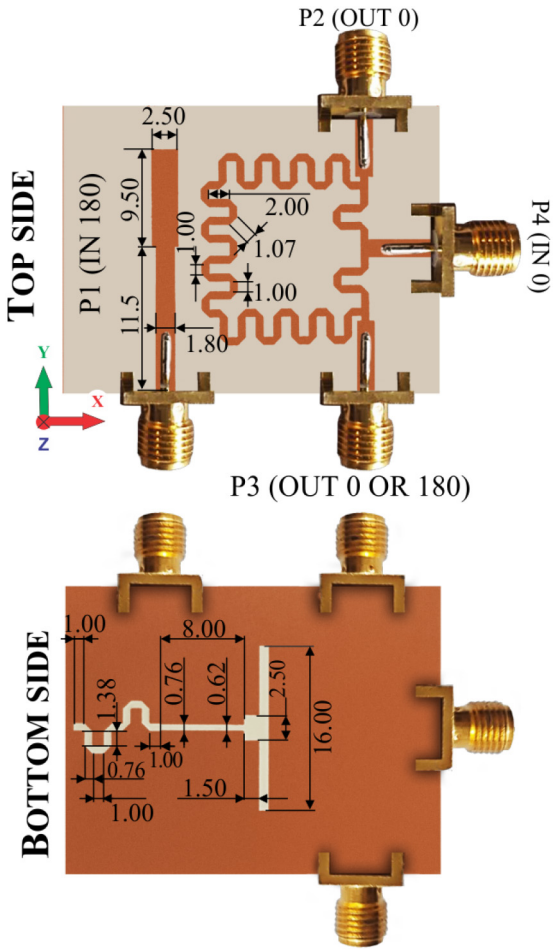


**FIGURE 14.** Top and bottom view of the manufactured slot-line meandered hybrid coupler. Coupler port 1 provides a differential phase shift at the output, while port 4 provides an equal phase shift. Final dimensions of the coupler are defined in millimeters.

the realized gain approaches 12 dBi. In addition, isolation values are about 70 dB at the coupler ports (see Table 7).

The array also offers FD beam steering capabilities. The normalized beam patterns can be see in Fig. 21 at 2.3 GHz. Other characteristics for the FD array are outlined in Table 6. For beam steering in the $-y$ direction, the phases of the ports for antenna port 1 (AP1), and AP2, AP5, as well as AP6 (see Fig. 18) must remain as 0° and 180° for each element, while for AP9, AP10, AP13 and AP14 the phase applied is outlined in Table 6. It should be noted that for about a 65°

**TABLE 6.** Full-duplex antenna array characteristics considering different steered beam positions in the *y-z* plane.

| | 2.2 GHz | | | | 2.3 GHz | | | | 2.4 GHz | | | |
|---|---|---|---|---|---|---|---|---|---|---|---|---|
| Applied Phase | Beam Position | Max. Realized Gain (dBi) | SLL (dB) | Cross-pol. below Beam Max (dB) | Beam Position | Max. Realized Gain (dBi) | SLL (dB) | Cross-pol. below Beam Max (dB) | Beam Position | Max. Realized Gain (dBi) | SLL (dB) | Cross-pol. below Beam Max (dB) |
| 0° | 0° | 11 | <30 | -54 | 0° | 11.8 | <30 | -50.1 | 0° | 11.1 | <30 | -44 |
| 20° | -4° | 11 | <30 | -52 | -4° | 11.7 | -23 | -50 | -3° | 11 | -22.1 | -43 |
| 45° | -10° | 10.9 | -21 | -52 | -9° | 11.6 | -21 | -52 | -8° | 10.8 | -16 | -44.5 |
| 65° | -14° | 10.7 | -14 | -53 | -13° | 11.4 | -11.4 | -50.7 | -12° | 10.6 | -11.4 | -45 |
| 90° | -21° | 10 | -8.3 | -52 | -21° | 10.8 | -8.3 | -50 | -20° | 10 | -7 | -44 |
| 110° | -23° | 10 | -7.6 | -54 | -22° | 10.8 | -6.9 | -49 | -23° | 9.9 | -5.9 | -45 |

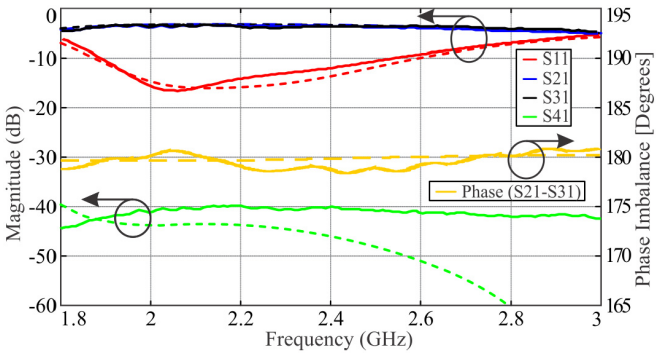


**FIGURE 15.** Simulated (dashed lines) and measured (sold lines) coupler response considering Port 1 as the input which provides a differential phase output.

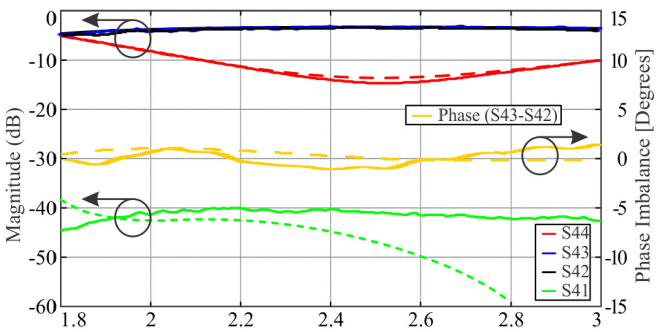


**FIGURE 16.** Simulated (dashed lines) and measured (solid lines) coupler response considering Port 4 as the input which provides an equal phase output.

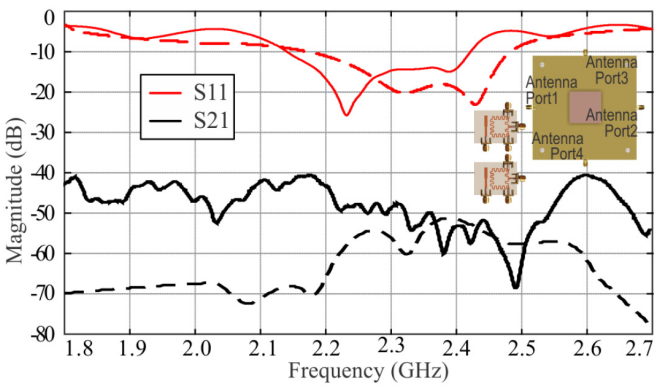


**FIGURE 17.** Simulated (dashed lines) and measured (solid lines) S-parameters of the antenna (nylon screws prototype, Fig. 9) with the newly proposed slot-line coupler (Fig. 14). Simulations are inline with the measurements which used the same experimental setup as outlined for Fig. 8.

phase shift at the ports, the sidelobe level (SLL) performance needs to be taken into account. In addition, for an increased shift of 90°, the SLL reaches −7 dB at 2.4 GHz. It should

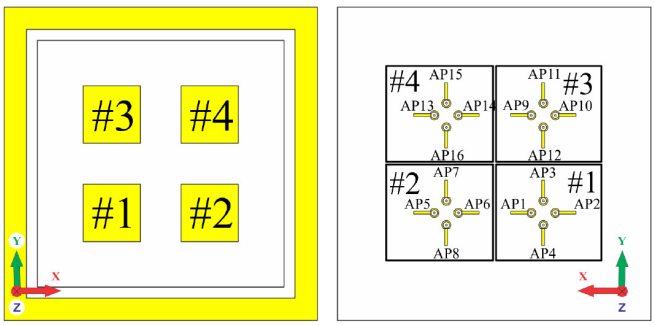


**FIGURE 18.** Top and bottom view of the proposed FD array. The bottom feeding system was modified to reduce the length of the connecting feeding system.

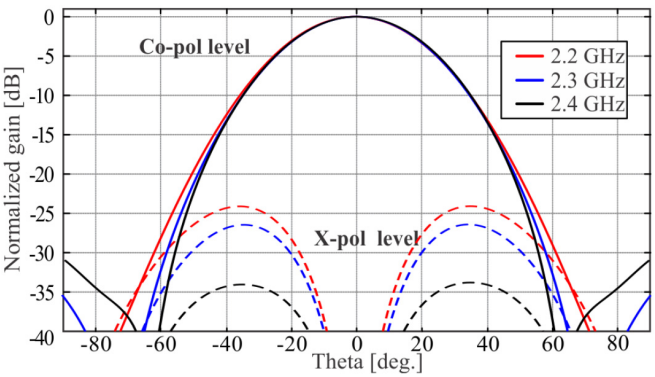


**FIGURE 19.** Simulated beam patterns of the FD array system. It should be noted that polarization purity at boresight is better in comparison to the single-element; i.e., values are more than 40 dB from the main co-pol. maximum.

be mentioned that cross-polarization levels are well below 40 dB (from the main beam maximum) over all simulated beam steering responses.

To further investigate the 2×2 array element coupling, the antenna system was simulated with a set of 8 hybrid couplers (see Fig. 22). The combined S-parameters showed that the cross-coupling between the elements are highest for AP1+AP2 and AP9+AP10 (which relate to antenna elements #1 and #3 indicative of the same polarization) which was at most −20 dB (see $S_{31}$ in Fig. 23). However, for the orthogonal polarization, which is important when considering FD operation, coupling between AP1+AP2 and AP7+AP8 (which relate to antenna elements #1 and #2) approaches −30 dB (see $S_{71}$ in Fig. 23). Similar responses were observed for the other antenna elements due to symmetry of the array. These results suggest that the antenna is capable of FD beam steering but that additional coupling

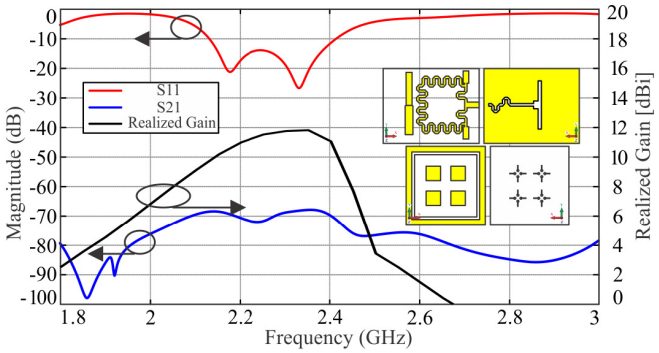


**FIGURE 20.** Combined simulation of the slot-line hybrid couplers and the FD antenna array (see inset of the models) for broadside radiation; i.e., no beam steering and no phase shifters as in Fig. 19. The two port setup consists of two slot-line couplers and 12 Wilkinson power dividers connected to the antenna ports (AP) as outlined in Fig. 18 where S-parameter results are defined at port 1 for the two couplers. It should be mentioned that simulations do not include the response of the connecting cables.

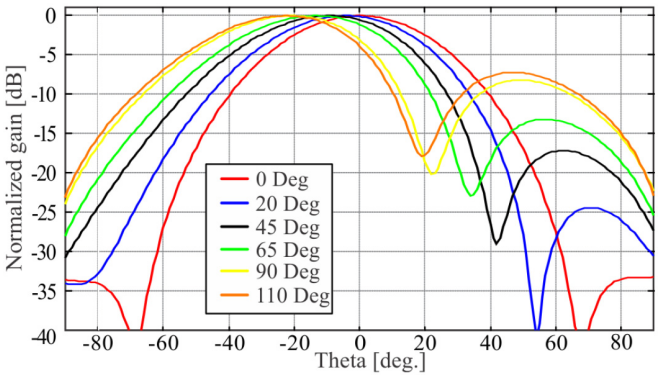


**FIGURE 21.** Simulated beam steering capabilities in the *y-z* plane for the 2×2 array at 2.3 GHz using the considered phase shift definitions as in Table 6.

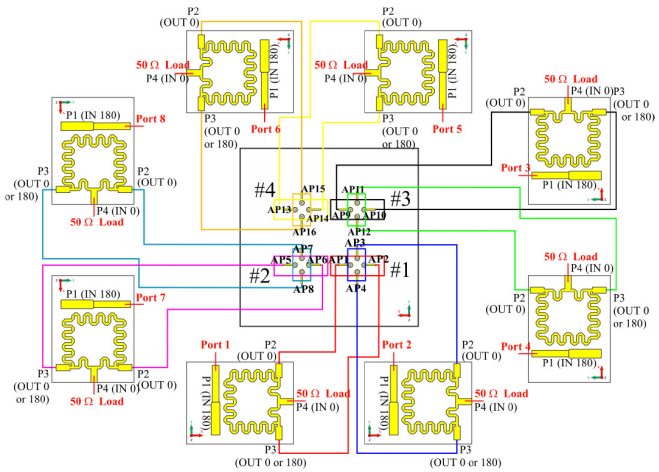


**FIGURE 22.** Architecture to model the coupling for the elements within the array. It should be noted that to feed such a system, 8 couplers will be required (see Table 7, option 2).

reduction approaches might be required depending on the isolation levels needed. The remaining S-parameter results for all elements are presented in Fig. 23.

From these findings and the architecture of the array it should be identified that such a beam steering antenna system

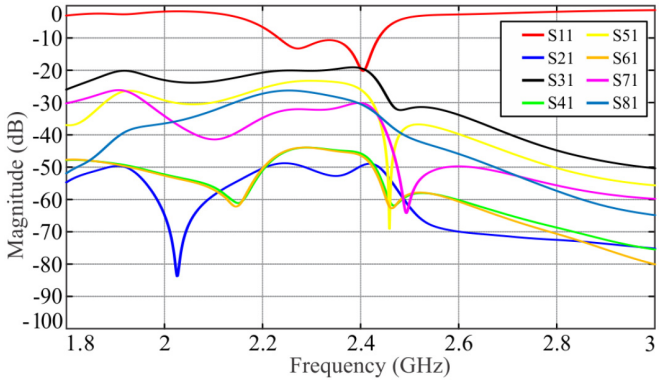


**FIGURE 23.** Simulated S-parameter response considering the setup as in Fig. 22. It should be mentioned that the highest coupling of about −20 dB can be observed between AP1+AP2 and AP9+AP10 which have the same polarization. The coupling for the worst case for the elements which generate orthogonal polarization; i.e., $S_{71}$, can be seen for AP1+AP2 to AP7+AP8 which is around −30 dB at 2.4 GHz.

**TABLE 7.** Array feeding configurations enabling FD operation considering broadside radiation and ideal phase shifters.

| Array Options | Number of Slot-line Couplers | Number of Phase Shifters | Number of Power Dividers | Element Isolation |
|---|---|---|---|---|
| 2-port | 2 | 16 | 12 | >60 dB (see Fig. 20) |
| 8-port | 8 | 8 | 0 | >30 dB (see Fig. 23) |

can be fed in two different ways: 1) as a two-port system when only two couplers and a set of power dividers employed with the response presented in Fig. 20, and, 2) as an 8-port system using 8 couplers to feed each element as depicted in Fig. 22 with responses in Fig. 23. These proposed feeding options and some results are presented in Table 7. Other feeding systems are possible as well.

Depending on the configuration, the number of couplers and phase shifters for beam steering can vary. Option 1 achieves excitation using dividers, requiring 2 hybrid couplers and 16 phase shifters for beam steering. Similarly for the 8-port configuration (Option 2), 8 couplers and 8 phase shifters will be required. Depending on the feeding architecture for the array, these two different feeding options are possible and the one that requires less phase shifters may be preferable due to the possible cost savings, however, improved isolation values (more than 60 dB) are observed with the 2-port implementation at the external feed network ports.

## VI. CONCLUSION

In this paper a new IBFD dual-polarized antenna element and 2×2 array were presented for S-band applications. Two different single-element prototypes based on foam spacers and nylon screws were discussed and the presented designs offer improvements in terms of isolation and bandwidth when compared to similar structures previously reported (see Table 3). Two simple external hybrid-couplers were manufactured and used with the combined antenna system. The measured single element isolation was around 45 dB for the foam spacer and approached 70 dB for the nylon screw system complimenting the design approach. Most notably, a meandered slot-line based coupler to reduce the magnitude and phase imbalances feeding the antenna was also

demonstrated, and this coupler offers better performances when compared to other structures in the literature in terms of bandwidth, isolation, and reduced coupler imbalances (see Table 4). A 2×2 array was also proposed for FD beam steering applications and two different options for feeding the array were investigated. The array offers similar matching to the single-element antenna, showing almost 12 dBi of realized gain and cross-polarization levels below 50 dB.

The antenna isolation might be improved by considering a larger ground plane, mainly to increase gain and reduce any leakage currents and unwanted coupling to the feeding system and network analyzer. Basically, an increase in ground plane size might improve practical isolation levels, however, our aim was to achieve a compact structure which is competitive in size when compared to other FD antenna systems as found in the literature. Improved operating bandwidths for the antenna might also be possible with a third patch layer, however, misalignment could be a practical issue for the multi-layer design. Additionally, the developed differential feed circuits could be integrated within the proposed antenna system to avoid the need of external cables. This attractive solution for future work would hopefully minimize any phase imbalances introduced by the many required mechanical cable connections. Ideally this effort for complete feed circuit integration when considering the developed differential couplers required for FD operation, would also improve the practical inter-port isolation levels.

## REFERENCES

[1] C. D. Nwankwo, L. Zhang, A. Quddus, M. A. Imran, and R. Tafazolli, "A survey of self-interference management techniques for single frequency full duplex systems," *IEEE Access*, vol. 6, pp. 30242–30268, 2018.

[2] J. M. B. da Silva, G. Fodor, and C. Fischione, "On the spectral efficiency and fairness in full-duplex cellular networks," in *Proc. IEEE Int. Conf. Commun. (ICC)*, 2017, pp. 1–6.

[3] D. Wen, G. Yu, R. Li, Y. Chen, and G. Y. Li, "Energy- and spectral-efficiency tradeoff in full-duplex communications," in *Proc. IEEE Globecom Workshops (GC Wkshps)*, 2016, pp. 1–6.

[4] J. Xue *et al.*, "Transceiver design of optimum wirelessly powered full-duplex MIMO IoT devices," *IEEE Trans. Commun.*, vol. 66, no. 5, pp. 1955–1969, May 2018.

[5] B. Debaillie *et al.*, "Analog/RF solutions enabling compact full-duplex radios," *IEEE J. Sel. Areas Commun.*, vol. 32, no. 9, pp. 1662–1673, Sep. 2014.

[6] Y. K. Chan, V. Koo, B.-K. Chung, and H.-T. Chuah, "A cancellation network for full-duplex front end circuit," *Progr. Electromagn. Res. Lett.*, vol. 7, pp. 139–148, 2009.

[7] Q. Zeng, Y. Zheng, B. Zhong, and Z. Zhang, "Minimum transmission protocol for full-duplex systems with energy harvesting," *IEEE Commun. Lett.*, vol. 23, no. 2, pp. 382–385, Feb. 2019.

[8] E. Ahmed and A. M. Eltawil, "All-digital self-interference cancellation technique for full-duplex systems," *IEEE Trans. Wireless Commun.*, vol. 14, no. 7, pp. 3519–3532, Jul. 2015.

[9] C.-X. Mao, S. Gao, and Y. Wang, "Dual-band full-duplex Tx/Rx antennas for vehicular communications," *IEEE Trans. Veh. Technol.*, vol. 67, no. 5, pp. 4059–4070, May 2018.

[10] L. Sun, Y. Li, Z. Zhang, and Z. Feng, "Compact co-horizontally polarized full-duplex antenna with omnidirectional patterns," *IEEE Antennas Wireless Propag. Lett.*, vol. 18, no. 6, pp. 1154–1158, Jun. 2019.

[11] D. Bharadia, E. Mcmilin, and S. Katti, "Full duplex radios," *ACM SIGCOMM Comput. Commun. Rev.*, vol. 43, no. 4, pp. 375–386, 2013.

[12] M. Duarte, C. Dick, and A. Sabharwal, "Experiment-driven characterization of full-duplex wireless systems," *IEEE Trans. Wireless Commun.*, vol. 11, no. 12, pp. 4296–4307, Dec. 2012.

[13] M. Chung, M. S. Sim, J. Kim, D. K. Kim, and C. Chae, "Prototyping real-time full duplex radios," *IEEE Commun. Mag.*, vol. 53, no. 9, pp. 56–63, Sep. 2015.

[14] K.-L. Wong, H.-C. Tung, and T.-W. Chiou, "Broadband dual-polarized aperture-coupled patch antennas with modified H-shaped coupling slots," *IEEE Trans. Antennas Propag.*, vol. 50, no. 2, pp. 188–191, Feb. 2002.

[15] J. Li, D. Wu, G. Zhang, Y. Wu, and C. Mao, "Compact dual-polarized antenna for dual-band full-duplex base station applications," *IEEE Access*, vol. 7, pp. 72761–72769, 2019.

[16] A. Sabharwal, P. Schniter, D. Guo, D. W. Bliss, S. Rangarajan, and R. Wichman, "In-band full-duplex wireless: Challenges and opportunities," *IEEE J. Sel. Areas Commun.*, vol. 32, no. 9, pp. 1637–1652, Sep. 2014.

[17] R. Lian, T.-Y. Shih, Y. Yin, and N. Behdad, "A high-isolation, ultra-wideband simultaneous transmit and receive antenna with monopole-like radiation characteristics," *IEEE Trans. Antennas Propag.*, vol. 66, no. 2, pp. 1002–1007, Feb. 2018.

[18] E. Yetisir, C.-C. Chen, and J. L. Volakis, "Wideband low profile multiport antenna with omnidirectional pattern and high isolation," *IEEE Trans. Antennas Propag.*, vol. 64, no. 9, pp. 3777–3786, Sep. 2016.

[19] H. Nawaz and I. Tekin, "Compact dual-polarised microstrip patch antenna with high interport isolation for 2.5GHz in-band full-duplex wireless applications," *IET Microw. Antennas Propag.*, vol. 11, no. 7, pp. 976–981, 2017.

[20] H. Nawaz and I. Tekin, "Double-differential-fed, dual-polarized patch antenna with 90 dB interport RF isolation for a 2.4 GHz in-band full-duplex transceiver," *IEEE Antennas Wireless Propag. Lett.*, vol. 17, no. 2, pp. 287–290, Feb. 2018.

[21] Y. Zhang, S. Zhang, J.-L. Li, and G. F. Pedersen, "A dual-polarized linear antenna array with improved isolation using a slotline-based 180ř hybrid for full-duplex applications," *IEEE Antennas Wireless Propag. Lett.*, vol. 18, no. 2, pp. 348–352, Feb. 2019.

[22] J. Ha, M. A. Elmansouri, P. V. Prasannakumar, and D. S. Filipovic, "Monostatic co-polarized full-duplex antenna with left- or right-hand circular polarization," *IEEE Trans. Antennas Propag.*, vol. 65, no. 10, pp. 5103–5111, Oct. 2017.

[23] R. B. Waterhouse, "Design of probe-fed stacked patches," *IEEE Trans. Antennas Propag.*, vol. 47, no. 12, pp. 1780–1784, Dec. 1999.

[24] Z. Zhou, Y. Li, J. Hu, Y. He, Z. Zhang, and P.-Y. Chen, "Monostatic copolarized simultaneous transmit and receive (STAR) antenna by integrated single-layer design," *IEEE Antennas Wireless Propag. Lett.*, vol. 18, no. 3, pp. 472–476, Mar. 2019.

[25] H. Saeidi-Manesh, S. Saeedi, and G. Zhang, "Dual-polarized perpendicularly fed balanced feed antenna with high polarization purity," *IEEE Antennas Wireless Propag. Lett.*, vol. 19, no. 2, pp. 368–372, Feb. 2020.

[26] N. A. Nguyen *et al.*, "Dual-polarized slot antenna for full-duplex systems with high isolation," *IEEE Trans. Antennas Propag.*, early access, Jul. 27, 2020, doi: 10.1109/TAP.2020.3010959.

[27] D. M. Pozar, *Microwave Engineering*, 3rd ed. Hoboken, NJ, USA: Wiley, 2005.

[28] L. Fan, C.-Hsun Ho, S. Kanamaluru, and K. Chang, "Wide-band reduced-size uniplanar magic-T, hybrid-ring, and de Ronde's CPW-slot couplers," *IEEE Trans. Microw. Theory Techn.*, vol. 43, no. 12, pp. 2749–2758, Dec. 1995.

[29] K. U-yen, E. J. Wollack, J. Papapolymerou, and J. Laskar, "A broadband planar magic-T using microstrip-slotline transitions," *IEEE Trans. Microw. Theory Techn.*, vol. 56, no. 1, pp. 172–177, Jan. 2008.

[30] M. Caillet, M. Clenet, A. Sharaiha, and Y. M. M. Antar, "A compact wide-band rat-race hybrid using microstrip lines," *IEEE Microw. Wireless Compon. Lett.*, vol. 19, no. 4, pp. 191–193, Apr. 2009.

[31] W. Feng, W. Che, and K. Deng, "Compact planar magic-T using E-plane substrate integrated waveguide (SIW) power divider and slotline transition," *IEEE Microw. Wireless Compon. Lett.*, vol. 20, no. 6, pp. 331–333, Jun. 2010.

[32] G. Brzezina and L. Roy, "Miniaturized 180° hybrid coupler in LTCC for L-band applications," *IEEE Microw. Wireless Compon. Lett.*, vol. 24, no. 5, pp. 336–338, May 2014.

[33] H. Liu, S. Fang, and Z. Wang, "Modified coupled line trans-directional coupler with arbitrary power divisions and its application to a 180° hybrid," *IET Microw. Antennas Propag.*, vol. 9, no. 7, pp. 682–688, 2015.

**MAKSIM V. KUZNETCOV** (Graduate Student Member, IEEE) was born in Kopeysk, Russia, in 1993. He received the M.Eng. degree in electrical and electronic engineering from Heriot-Watt University, Edinburgh, U.K., in 2019. He is currently pursuing the Ph.D. degrees with Heriot-Watt University (HWU), Edinburgh, and the University of Edinburgh (UoE), Edinburgh.

In 2019, he joined HWU and UoE as an Research Student, where his research interests include the analysis and design of leaky-wave antennas, duplex and polarization-diverse antenna systems, and other microwave, and antenna technologies.

**SYMON K. PODILCHAK** (Member, IEEE) received the B.A.Sc. degree in engineering science from the University of Toronto, Toronto, ON, Canada, in 2005, the M.A.Sc. and Ph.D. degrees in electrical engineering from Queen's University, Kingston, in 2008 and 2013, respectively.

From 2013 to 2015, he was an Assistant Professor with Queen's University. In 2015, he joined Heriot-Watt University, Edinburgh, U.K., as an Assistant Professor, and became an Associate Professor in 2017. He is currently a Senior Lecturer with the School of Engineering, The University of Edinburgh, Edinburgh. He is also a registered Professional Engineer (P.Eng.) and has had industrial experience as a Computer Programmer, and has designed 24 and 77 GHz automotive radar systems with Samsung and Magna Electronics. Recent industry experience also includes the design of high frequency surface-wave radar systems, professional software design and implementation for measurements in anechoic chambers for the Canadian Department of National Defence and the SLOWPOKE Nuclear Reactor Facility. He has also designed compact antennas for wideband military communications, highly compact circularly polarized antennas for CubeSats with COM DEV International and The European Space Agency ESA, and new wireless power transmission systems for Samsung. His research interests include surface waves, leaky-wave antennas, metasurfaces, UWB antennas, phased arrays, and RF integrated circuits.

Dr. Podilchak and his students have been the recipient of many best paper awards and scholarships; most notably Research Fellowships from the IEEE Antennas and Propagation Society (AP-S), the IEEE Microwave Theory and Techniques Society (MTT-S), and the European Microwave Association. He also received a Postgraduate Fellowship from the Natural Sciences and Engineering Research Council of Canada (NSERC), five Young Scientist Awards from the International Union of Radio Science URSI, and the Outstanding Dissertation Award for his Ph.D from Queen's University. In 2011, 2013, and 2020, student paper awards were received at the IEEE International Symposium on Antennas and Propagation, and in 2012, the Best Paper Prize for Antenna Design at the European Conference on Antennas and Propagation for his work on CubeSat antennas, and in 2016, he received the European Microwave Prize for his research on surface waves and leaky-wave antennas. In 2017 and 2019, he was bestowed a Visiting Professorship Award at Sapienza University, Rome, Italy, and from 2016 to 2019 his research was supported by a H2020 Marie Sklodowska-Curie European Research Fellowship. He was recognized as an Outstanding Reviewer for the IEEE TRANSACTIONS ON ANTENNAS AND PROPAGATION in 2014 and 2020. He was also the Founder and a First Chairman of IEEE AP-S and IEEE MTT-S Joint Chapters in Canada and Scotland. In recognition of these services, he was presented with an Outstanding Volunteer Award from IEEE. He has been a Lecturer for the European School of Antennas and an Associate Editor for *IET Electronics Letters*. He currently serves as a Guest Associate Editor for IEEE OPEN JOURNAL OF ANTENNAS AND PROPAGATION and IEEE ANTENNAS AND WIRELESS PROPAGATION LETTERS.

**ARIEL J. MCDERMOTT** (Student Member, IEEE) was born in Hexham, U.K., in 1996. He received the master's degree in electrical and electronics engineering from Heriot-Watt University in Edinburgh, U.K., in 2019. He is currently working in the U.K. defense sector. His primary research area consists of RF, microwave and antenna engineering.

**MATHINI SELLATHURAI** (Senior Member, IEEE) is currently a Professor of signal processing and wireless communications with Heriot-Watt University, Edinburgh, U.K. She has been active in signal processing research for the past 20 years and has a strong international track record in multiple-input, multiple-output (MIMO) signal processing with applications in radar, and wireless communications. She held visiting positions with Bell-Laboratories, Holmdel, NJ, USA, and at The Canadian Communications Research Centre, Ottawa, Canada. She has published over 200 peer reviewed papers in leading international journals and IEEE conferences, given invited talks and has written several book chapters as well as a research monograph as a lead author. Her present research includes full-duplex systems, passive radar topography, localisation, massive-MIMO, non-orthogonal multiple access, waveform designs, caching technologies, assisted care technologies, IoT, hearing-aids, optimal coded-modulation designs using auto-encoders, channel prediction, and mm-wave imaging and communications.

She is a recipient of an IEEE Communication Society Fred W. Ellersick Best Paper Award in 2005, the Industry Canada Public Service Awards for contributions to Science and Technology in 2005, and Awards for contributions to Technology Transfers to Industry in 2004. She was the recipient of the Natural Sciences and Engineering Research Council of Canada (NSERC) Doctoral Award for her Ph.D. dissertation in 2002. She was an Editor for IEEE TRANSACTIONS ON SIGNAL PROCESSING from 2009 to 2014, and from 2015 to 2018, the General Co-Chair of IEEE SPAWC2016 in Edinburgh, and a member for IEEE SPCOM Technical Strategy Committee from 2014 to 2019.